Solid-State NMR Identification and Quantification of Newly Formed Aluminosilicate Phases in Weathered Kaolinite Systems

Garry S. Crosson,[†] Sunkyung Choi,[‡] Jon Chorover,[‡] Mary Kay Amistadi,[‡] Peggy A. O'Day,[§] and Karl T. Mueller*[,†]

Department of Chemistry, The Pennsylvania State University, University Park, Pennsylvania 16802, Department of Soil, Water and Environmental Science, University of Arizona, Tucson, Arizona 85721, and School of Natural Sciences, University of California, Merced, California 95344

Received: September 22, 2005; In Final Form: November 15, 2005

The weathering of a specimen kaolinite clay was studied over the course of 369 d via solid-state ^{29}Si magic angle spinning (MAS) nuclear magnetic resonance (NMR) spectroscopy and high-field ^{27}Al MAS NMR. The chosen baseline solution conditions (0.05 mol kg^{-1} of Al, 2 mol kg^{-1} of Na^+, 1 mol kg^{-1} of NO_3^-, 1 mol kg^{-1} of OH^-, and pH ∼13.8) approximate those of solutions leaking from waste tanks at the Hanford Site in Richland, WA. Nonradioactive Cs and Sr cations were added to this synthetic tank waste leachate (STWL) solution at concentrations of 10^{-3}, 10^{-4}, and 10^{-5} molal (*m*) to represent their radionuclide counterparts. The transformations of silicon- and aluminum-containing solid phase species were monitored quantitatively by using NMR spectroscopy, with the resulting spectra directly reporting the influence of the initial Cs and Sr on formation and transformation of the neo-formed solids. At the lowest concentration of Cs and Sr employed (10^{-5} *m* in each cation) peaks consistent with the formation of zeolite-like minerals were detected via ^{29}Si and ^{27}Al MAS NMR as early as 33 d. At concentrations of 10^{-3} *m* in each cation, new silicon species are not detected until 93 d, although neophases containing four-coordinate aluminum were detectable at earlier reaction times via ^{27}Al MAS NMR. At the highest magnetic field strengths employed in this NMR study, deconvolutions of resonances detected in the tetrahedral region of the ^{27}Al MAS spectra yielded multiple components, indicating the existence of at least four new aluminum-containing phases. Two of these phases are identified as sodalite and cancrinite through comparison with diffuse-reflectance infrared (DRIFT) spectra and powder X-ray diffraction (XRD) results, while a third phase may correlate with a previously detected aluminum-rich chabazite phase. All measurable solid reaction products have been quantified via their ^{27}Al MAS resonances acquired at high magnetic field strengths (17.6 T), and the quantitative nature of the ^{27}Al NMR data shows that cancrinite growth increases while sodalite reaches a steady state with respect to total aluminum in the solid phases. The data also relate the coupling of Cs sorption to the ripening of feldspathoid phases in this heterogeneous system as a function of time, and illustrate the important influence of co-contaminants on the environmental reaction kinetics studied here.

Introduction

A lasting legacy of the United States' production of nuclear materials has been the stockpiling of many millions of gallons of highly radioactive waste, the bulk of which is stored at the Hanford Site along the Columbia River in Washington State.[1] Presently, approximately 54 million gallons of high level radioactive and chemical wastes are stored within 177 stainless steel-lined underground tanks at Hanford. Waste-induced tank corrosion resulted in the release of more than a million gallons of waste (from 67 storage tanks) into the adjoining soil and groundwater. To mitigate corrosion, an attempt was made to neutralize the initially acidic waste solution.[1] As a result, caustic (pH >13) sludge formed, containing metal oxides and hydroxides along with highly soluble cations such as Sr^{2+} and Cs^+, which account for the bulk of the radioactivity.[2] The radioactive leachates contain molar amounts of hydroxide, and high ionic concentrations of sodium, aluminate, and nitrate. These tank waste leachates enter the vadose zone and can interact with soil components, including secondary clay minerals such as kaolinite and montmorillonite. ^{90}Sr and ^{137}Cs both have radioactive half-lives of approximately 30 y, are likely mobile in groundwater, and have chemistries that result in the replacement of important cations in living organisms. Hence, knowledge of their transport and fate in the environment is an important consideration in the generation of reliable containment and remediation strategies.

Currently, it is known that hydroxide-induced mineral dissolution occurs under the conditions present at the Hanford site,[3−5] and that these conditions favor the formation of porous aluminosilicate phases. In earlier studies, Bickmore et al. found that nitrate-cancrinite precipitated onto quartz sand surfaces at 89 °C and at solution pH values of 11.3 and 12.4.[4] However, until recent work from our team,[6] no investigation studying the effects of Cs and Sr on the dissolution/formation processes had been presented. Apart from this earlier study, little is known about the effects of Cs and Sr cations on mineral dissolution/formation processes at Hanford under environmentally relevant conditions.

* To whom correspondence should be addressed, E-mail address: ktm2@psu.edu.
[†] The Pennsylvania State University.
[‡] University of Arizona.
[§] University of California.

10.1021/jp055401l CCC: $33.50
Published on Web 12/21/2005

High-resolution solid-state NMR spectroscopy is a powerful method for studying heterogeneous systems, providing isotope-specific sensitivity for probing local structure and dynamics. Previous NMR studies of mineral systems have provided information about mineral crystallinity, cation binding sites, coordination numbers, and mineral dissolution reaction kinetics.[6−8] For secondary minerals such as kaolinite, a number of recent studies provide insight into the processes investigated here. For example, ^{29}Si NMR indicated that silica-alumina and amorphous silica form upon dealumination of kaolinite at elevated temperature;[8] the formation of hydroxy-sodalite and zeolite A from kaolinite dissolution under strongly alkaline conditions was observed via ^{27}Al and ^{29}Si solid-state NMR studies;[9] and our collaborative studies have utilized ^{27}Al solid-state NMR to follow the loss of six-coordinate aluminum species in kaolinite clay subjected to a simulated tank waste leachate and reveal that kaolinite dissolution could be modeled by first-order kinetics.[6] Although solid-state NMR of alkaline dissolution of kaolinite clays has been previously studied, no comprehensive study of the kinetics of formation of neophases has been reported. Clearly, this knowledge is necessary to refine and increase the predictive capabilities of models, where such studies provide, for example, rate information for modeling of reactive transport and sequestration of radionuclides in the vadose zone. Here, we present a comprehensive ^{29}Si and high-field ^{27}Al NMR study of the hydroxide-promoted dissolution of kaolinite in the presence of Cs and Sr cations, focused on the subsequent production of new aluminosilicate phases. In particular, we consider the effects of the concentrations of (nonradioactive) Cs and Sr contaminant surrogates on kaolinite dissolution and neophase formation kinetics under the extreme chemical conditions of a simulated tank waste leachate (STWL) solution.

Experimental Section

Sample Preparation. Kaolinite (Washington County, Georgia) was obtained from the Source Clay Minerals Repository at the University of Missouri. A detailed description of the kaolinite purification, preparation, and characterization via powder X-ray diffraction is provided elsewhere.[6] The structural formula of this purified kaolinite, obtained via total elemental analysis, was $[Si_4]Al_{3.66}Fe(III)_{0.07}Ti_{0.06}O_{10}(OH)_8$. Kaolinite fractions with particle sizes $<2\ \mu$m were used in all studies reported here. Weathering experiments were performed with a solution containing 0.05 mol kg^{-1} of total Al, 2 mol kg^{-1} of Na^+, 1 mol kg^{-1} of NO_3^-, and 1 mol kg^{-1} of OH^-, The pH of the initial solution was approximately 14. The STWL was spiked with Cs^+ and Sr^{2+} co-contaminants at concentrations of 10^{-5}, 10^{-4}, and 10^{-3} mol kg^{-1} of each cation. Weathering experiments were conducted in batch mode, using ultrapure (MilliQ) water in 50-mL polypropylene copolymer (PPCO) bottles. Each reactor contained 0.5 g dry mass of clay suspended in 25.0 g of STWL solution, for a solid-to-solution ratio of 1:50. Six replicate reactors were used for each time point comprising duplicate sets for (i) wet chemistry analysis, (ii) NMR analysis after reaction, and (iii) NMR analysis after postreaction acidic ammonium oxalate (AAO) extractions.[6]

An end over end shaker was utilized to agitate the samples at 2 rpm for 1, 7, 33, 93, 190, and 369 d. Clay suspensions were transferred to PPCO centrifuge tubes and centrifuged at 28 700 *g* for 20 min at the termination of a given reaction period. A 0.2-μm PTFE syringe filter was used to filter the supernatant solution, which was then acidified to pH 1−2 with trace metal grade concentrated HNO_3. Prior to analyses of the solids, entrained salt solution was removed by resuspending centrifuged pellets in 95% ethanol (adjusted to pH 10 with 1 M NaOH) followed by two additional ethanol washes. Immediately following this treatment, two samples were removed, dispersed in 15 mL of Milli-Q water, frozen at −80 °C, and subsequently freeze-dried for NMR (and other) analyses.

Remaining samples for solid-phase analyses were resuspended in 33 g of 0.1 M $Mg(NO_3)_2$, shaken for 1 h, and then centrifuged at 28 700 *g* for 20 min to extract readily exchangeable Cs and Sr. The supernatant was collected and acidified with concentrated HNO_3 to pH 2. To study the recalcitrance of neoformed solids to acid treatments, a portion of the reacted clays was subjected to an AAO extraction.[10] Three washes of pelletized samples were first accomplished with 95% ethanol; the pellets were then resuspended in 0.2 M AAO for 4 h at pH 3 on a reciprocal shaker in the dark to extract poorly crystalline precipitates. The samples were recentrifuged at 28 700 *g* for 20 min and the supernatant solution was acidified to pH 1. The remaining solids were successively washed with 0.1 and 0.01 M NaCl to remove AAO, followed by three washes with 95% ethanol prior to freeze-drying for NMR analysis.

NMR Experiments. *^{27}Al MAS NMR.* ^{27}Al MAS NMR experiments were performed at four different magnetic field strengths. The spectrometers utilized include a Chemagnetics CMX-300 spectrometer with a 7.0 T superconducting magnet (^{1}H resonance frequency of 300 MHz), a home-built spectrometer with a 9.4 T magnet and controlled by a Tecmag Libra pulse programming system (^{1}H resonance frequency of 400 MHz), a Varian/Chemagnetics Infinity-500 spectrometer with an 11.7 T magnet (^{1}H resonance frequency of 500 MHz), and a Varian Inova spectrometer with a 17.6 T magnet (^{1}H resonance frequency of 750 MHz) to which we were granted access at the Environmental Molecular Sciences Laboratory at Pacific Northwest National Laboratory. The lower frequency channel of a 4-mm Chemagnetics HX double-resonance MAS probe, operating at frequencies of 78.49 and 104.29 MHz, was used for ^{27}Al experiments at 7.0 and 9.4 T, respectively. At 11.7 T, the lower frequency channel of a 5 mm Chemagnetics HX probe was used, operating at 130.19 MHz. Spectra were acquired at 17.6 T, using a Jacobsen 5 mm HX probe operating at 195.41 MHz. Single-pulse ^{27}Al-free induction decays were acquired after short radio frequency pulses of 0.8 μs (equivalent to a 15° tip angle for the central transition), utilizing spinning rates of 10.00−14.00 kHz at 7.0, 9.4, and 11.7 T, and a recycle delay of 1 s. In the highest field magnet (17.6 T), spinning speeds of 7.50 kHz were maintained and similar tip angle and relaxation delays were employed as at lower fields. Generally, the averaging of at least 4096 time domain acquisitions yielded good signal-to-noise ratios in the resulting frequency domain spectra. Free-induction decays of 1024, 2048, 4096, and 16396 data points were processed with an exponential windowing function corresponding to a line broadening of 50 Hz at 7.0, 9.4, 11.7, and 17.6 T, respectively. Spectra acquired at 17.6 T were also baseline corrected using an 8th order polynomial fitting function. The ^{27}Al shifts (in ppm) at all field strengths are externally referenced to the ^{27}Al resonance from a 1 M aqueous sample of $Al(H_2O)_6^{3+}$.

^{29}Si MAS NMR. ^{29}Si MAS NMR experiments were accomplished at 9.4 T with a home-built spectrometer based on a Tecmag Libra pulse programming and data acquisition system. A Chemagnetics triple channel transmission line probe with a 7.5-mm rotor was used for ^{29}Si one-pulse MAS experiments, with a ^{29}Si resonance frequency of 79.460 MHz. ^{29}Si MAS experiments were also performed at this magnetic field strength, using the middle frequency channel of a HXY 5 mm Chemag-

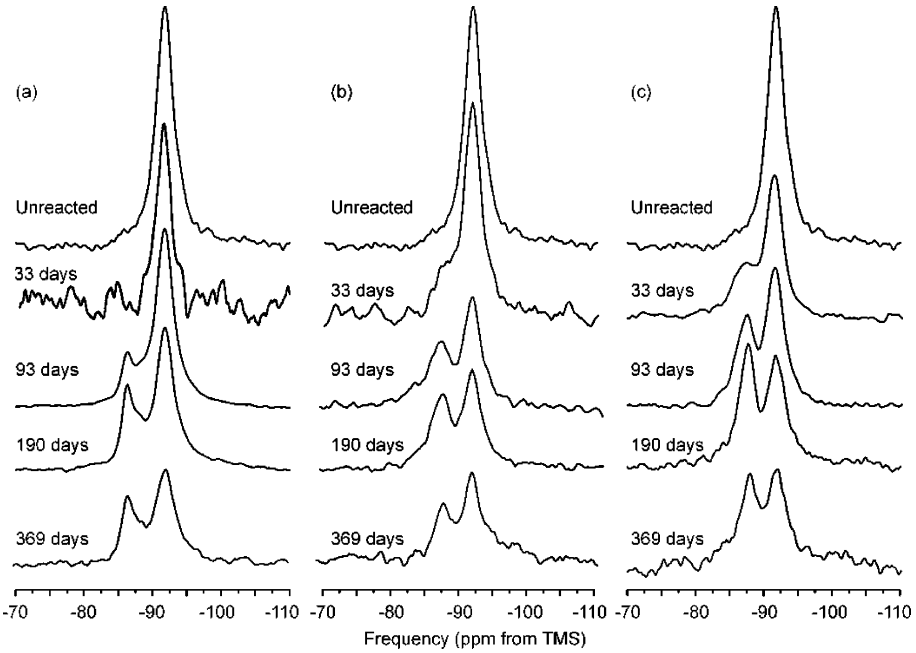

Figure 1. ^{29}Si MAS spectra of kaolinite reacted for various times with the synthetic tank waste leachate solution at Cs/Sr concentrations of (a) 10^{-3}, (b) 10^{-4}, and (c) 10^{-5} *m*.

netics MAS probe operating at a ^{29}Si resonance frequency of 79.460 MHz. Single-pulse ^{29}Si spectra were measured with use of radio frequency pulses of 7 μs (equivalent to a 90° tip angle), a spinning rate of 3.00 kHz, and a recycle delay of 60 s. Generally, 500−1200 time domain acquisitions yielded good signal-to-noise ratios in the frequency domain spectra. Free-induction decays of 4096 points were acquired, and subsequently processed with an exponential windowing function corresponding to a line broadening of 50 Hz. All time domain data sets were left shifted by three points to minimize or remove probe-ringing artifacts. Chemical shift values for ^{29}Si spectra were externally referenced to the ^{29}Si resonance from tetramethylsilane (TMS) at 0 ppm.

Results and Discussion

^{29}Si MAS NMR. Kaolinite is an aluminosilicate mineral composed of tetrahedral silicon oxide and octahedral aluminum oxide sheets in a 1:1 ratio. Figure 1 displays ^{29}Si MAS NMR spectra from the unreacted kaolinite sample as well as samples reacted with the STWL solutions for up to 369 d and across the studied concentration range of Sr and Cs co-contaminants. The spectrum for the unreacted mineral displays a single resonance for Q^3 silicon at −91.5 ppm, which is consistent with previously published work.[11] This spectrum was also satisfactorily fit with two Gaussian line shapes (fit not shown) at −91.2 and −91.6 ppm. In early ^{1}H/^{29}Si CPMAS studies of various kaolinite clays, two silicon environments were observed in experiments run at Larmor frequencies of 39.68, 59.61, and 79.50 MHz.[11,12] The results of these earlier ^{1}H/^{29}Si CPMAS NMR studies (as well as the current study) are in agreement with diffraction studies of kaolinite which suggest the presence of two silicon environments.[13] Our unsuccessful attempts to resolve these sites completely could result from the presence of paramagnetic impurities, or other sample specific conditions leading to broadening of the resonances.

Upon reaction of the kaolinite with the STWL solutions for 33 d, the spectra in Figure 1 reveal distinct changes in the local environments of a portion of the silicon in the samples. Since no additional silicon has been introduced via the STWL, these changes must correspond to changes in the environments of Si originally within the parent clay mineral phase, presumably due to release of silicon into solution followed by the formation of new solids. As reaction time increases, new resonances develop within the −85 to −90 ppm range, consistent with the growth of new four-coordinate silicate species. Neoformed phases containing quaternary silicon are detected as early as 33 d through resonances with maxima at −87.5 and −87.3 ppm for samples reacted with 10^{-4} and 10^{-5} *m* Cs and Sr co-contaminants, respectively. However, at the highest co-contaminant concentration (10^{-3} *m*), silicon-containing neophases are not detected until 93 d, and the resonance from this new phase has a maximum at −86.3 ppm. Beyond 93 d, new silicon species continued to form as more kaolinite dissolved or secondary reactions took place involving phases already precipitated from solution. As the reactions progressed, the centers of gravity of the resonances from these new species did not vary significantly, suggesting that rearrangements in the average silicon environment did not occur on the time scale of the reaction, or did not form substantially different silicon environments as evidenced by isotropic chemical shift values. However, the combined breadths of the original and neo-formed silicon resonances preclude full characterization or identification of the new phases as they form, other than a measure of relative concentrations of different silicate environments. In a concurrent diffraction study of these samples, sodium aluminum silicate (chabazite), sodium aluminum nitrate silicate (sodalite), along with sodium aluminum nitrate silicate hydrate (cancrinite) were identified as this reaction progressed,[6] concurrent with the observation of new resonances in the ^{27}Al MAS NMR spectra.

Cancrinite and sodalite are feldspathoid minerals that have zeolite-like characteristics and possess a three-dimensional channel structure that allows for intercalation of charge-balancing cations, anions, and water. Sodalite, with a cubic crystal system, and cancrinite, which has a hexagonal crystal system, have associated space groups of $P\bar{4}3n$ and $P6_3$, respectively.[14] The sodalite structure is composed of a body-centered cubic arrangement of β or sodalite cages linked via individual 4- and 6-ring openings.[14] The layer packing of the

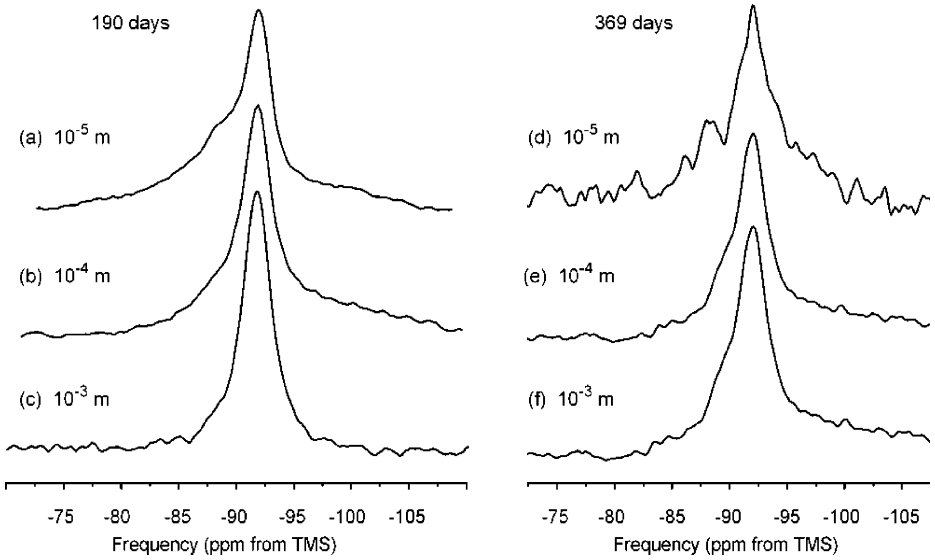

Figure 2. ^{29}Si MAS spectra of oxalate treated samples after 190 (a−c) and 369 d (d−f) reaction periods with the synthetic tank waste leachate at the indicated Cs/Sr concentrations.

hexagonal arrays of single 6-rings in the structure is ABCABC while the packing arrangement in cancrinite is of the ABAB type.[14] In contrast to cancrinite, sodalite lacks large, through-going channels due to its packing type. The channels of cancrinite and cages of both minerals are able to incorporate the charge-balancing ions, and both minerals consist of a perfectly alternating arrangement of SiO_4 and AlO_4 tetrahedra leading to Si/Al ratios of unity. Chabazite, a zeolite mineral, is composed of a series of interlinked double-6-ring units with an ABC stacking of the units[14,15] and has been reported to occur in nature with Si/Al ratios from 2 to 7.6 depending on the origin of the zeolite, the cation composition, and the degree of hydration.[16] The connected ring units form an open cage with six 8-ring pores, and this compound can be described by a *R*3*M* space group.

In the spectra of Figure 1, the new ^{29}Si resonances are not well resolved, but can be assigned to either sodalite or cancrinite if comparison is made with other studies where sodalite and cancrinite were synthesized with use of kaolinite as the silicon source.[9,17,18] In these systems, ^{29}Si MAS NMR resonances from sodalite and cancrinite were detected at −87.6 ppm where carbonate was the anion,[17] −86.5 ppm for hydroxy-sodalite,[9] −86.7 ppm for nitrate-sodalite,[19] −86.6 ppm for nitrate-cancrinite,[19] and −86.5 ppm for iodate-enclathrated sodalite.[20] Given the similar structures of cancrinite and sodalite, the ^{29}Si resonances for these Q^4(4Al) sites should possess very similar chemical shift values, and it was not possible to experimentally resolve and identify individual resonances as arising from specific mineral phases from the spectra in Figure 1. Hence, full or relative quantifications of each phase have not been attempted from ^{29}Si data.

Acid treatment of minerals is commonly used to prepare homogeneous clay mineral surfaces and to estimate the amorphous content of soils.[10,21,22] Acidic ammonium-oxalate treatments are highly selective for the dissolution of amorphous phases as well as acid-soluble phases such as zeolite (and related) minerals. Comparisons of AAO-treated clays after 190 and 369 d of STWL treatment at all three Cs and Sr concentrations are shown in Figure 2. The spectra indicate (via a decrease in the nonkaolinite peak intensities) that a substantial amount of material is indeed removed by the AAO treatment; the spectra also demonstrate that the amount of acid-removable phases decreases with increasing reaction time across the full concentration range of Cs and Sr co-contaminants. A comparison of the lowest and highest Cs/Sr concentrations at 190 d shows that the concentration of co-contaminants in the STWL solutions affects the amount of material that is removable through this treatment. At high concentrations, it is observed that the Q^3 resonance of kaolinite is the primary contributor to the spectral intensity after AAO treatment, while at low co-contaminant concentration the total remaining silicon is still contained in both Q^3 and Q^4 (neophase) sites. The above observations are consistent with previous X-ray data that showed complete removal of cancrinite and sodalite at high dosages and partial removal of neophases formed at lower concentrations.[6] A plausible explanation for incomplete removal at low contaminant concentrations is that the crystallinity of the neophases increased relative to the crystallinity at high concentrations, thus minimizing the effectiveness of the AAO treatment for dissolution of the material.[23] In addition, the spectra in Figure 2 acquired after 369 d of treatment at 10^{-4} and 10^{-5} *m* Cs and Sr show a shift in the neophase peak remaining after AAO treatment (here, the shoulder on the high-frequency side of the kaolinite peak) to a spectral position with lower (more negative) chemical shift value, indicating a different or altered phase for this recalcitrant material.

^{27}Al MAS NMR. Study of the aluminum transformation and speciation through ^{27}Al MAS NMR takes advantage of the wider dispersion of distinguishable shifts of ^{27}Al aluminum resonance lines in this system, but full separation of resonances is only possible at very high magnetic field strengths, as shown below. Figure 3 displays ^{27}Al MAS data for unreacted kaolinite (along with corresponding fits, deconvolutions, and residuals) from MAS experiments performed at 7.0, 9.4, and 11.7 T field strengths. The spectra were collected by using short radio frequency pulses to account for any difference in quadrupolar interaction parameters of different Al sites, and all spectra for kaolinite acquired in this study display a single asymmetric line in the region for six-coordinate aluminum species. Based on the observation of a shift in the center of gravity of the central transition as field strength is increased, the quadrupolar coupling constant, $C_q = e^2qQ/h$, is nonzero. As expected, the apparent degree of asymmetry then also decreases with increasing magnetic field strength, indicating a reduction in second-order quadrupolar broadening. In practice, measurement of the shift of the center of gravity of the central transition at multiple-

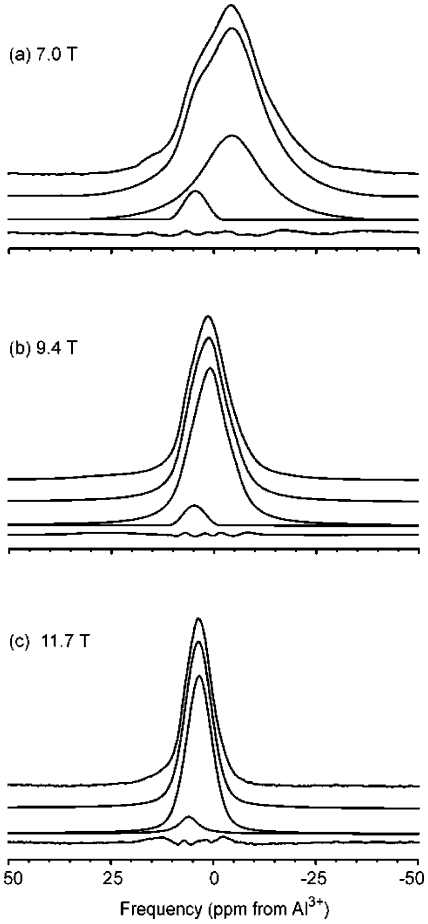

Figure 3. ^{27}Al Bloch decay spectra of unreacted kaolinite at (a) 7.0, (b) 9.4, and (c) 11.7 T. All spectra are displayed above a fit and the corresponding deconvolutions of each spectrum, with residuals from the fit at the bottom. All fits were performed with DMFIT2002.

field strengths yields the quadrupolar product, P_q, which also depends on the asymmetry parameter, η, for the quadrupolar tensor. P_q is defined as $P_q = C_q(1 + (\eta^2/3))^{1/2}$, and the observed center of mass of each ^{27}Al resonance (δ_{tot}^{cm}) contains contributions from the isotropic chemical shift value (δ_{cs}^{iso}) and the isotropic second-order quadrupolar shift (δ_{2Q}^{iso}), such that

$$\delta_{tot}^{cm} = \delta_{cs}^{iso} + \delta_{2Q}^{iso} = \delta_{cs}^{iso} - \frac{3}{40}\left(\frac{C_q}{\gamma B_0}\right)^2 \frac{(I(I+1) - {}^3/_4)}{I^2(2I-1)^2}\left(1 + \frac{\eta^2}{3}\right) \times 10^6 \quad (1)$$

where γ is the gyromagnetic ratio of the nucleus and I is the nuclear spin quantum number ($^5/_2$ for ^{27}Al). The total observed shift is dependent on the static magnetic field strength (B_0), and therefore P_q and δ_{cs}^{iso} are determined by plotting δ_{tot}^{cm} versus $1/B_0^2$. The spectra in Figure 3 were deconvoluted with DMFIT2002,[24] and the observed shifts for two separate components were tabulated at all fields and used to calculate δ_{cs}^{iso} and P_q. For a minor low-field (or high-frequency) component (site 1), the P_q and δ_{cs}^{iso} were found to be 1.84 MHz and 8.34 ppm, respectively. For site 2, δ_{cs}^{iso} and P_q were determined to be 8.64 ppm and 3.23 MHz, respectively, and are similar to values obtained by Hayashi and co-workers.[12] In the case of site 1, however, P_q differs from that reported by Hayashi and co-workers where they report P_q as 3.53 MHz. Presumably, site 1 is less distorted in the sample measured here due to differences in the clay origin or from pre- and posttreatment processing of the specimen. In any case, the percentage of site 1 in the clay has been reported to be no more than 5%, and this does not affect the calculations reported below to any substantial degree. Indeed, the low percentage of this site could also lead to some of the variation in parameters from those reported in the literature.

The formation of new phases containing four-coordinate aluminum species after the dissolution of clay minerals has been discussed previously in the literature.[25−28] Low-field ^{27}Al MAS NMR spectra of specimen kaolinite clays reacted for up to 369 d with the STWL solutions containing different Cs and Sr amounts were also published previously,[6] but in this previous study it was not possible to quantitate nor identify the phases contributing to the four-coordinate signal owing to the breadth of the resonance lines (in part due to second-order quadrupolar broadening effects) and the resulting spectral overlap.

In dynamic systems such as soils, where clay dissolution and zeolite-type mineral formation occurs, it is proposed that multiple phases form according to Ostwald's rule of transformation. This rule argues that the first phase to precipitate among those for which the solution is supersaturated will be that which exhibits the highest solubility and for which the solution is, therefore, closest to equilibrium saturation. At early reaction times, precipitates are thus normally disordered, but the crystallinity of the phases will generally increase with time. Evidence for this was presented in our previous work where nitrate-sodalite precipitates were not detected via XRD before 33 d although their presence was suggested by TEM and DRIFT data.[6] In the NMR spectra, broadening effects due to amorphous phases or low crystallinity in minerals should decrease with increasing reaction time, but the residual quadrupolar effects are still present and can be problematic at low fields. Therefore, new studies were carried out at 17.6 T on a spectrometer at the Pacific Northwest National Laboratory, Richland, WA. The results of ^{27}Al MAS NMR experiments performed at 17.6 T across the entire Cs and Sr concentration range are presented in Figure 4. Here, spectral resolution is superior to that obtained in our lower magnetic field strength studies allowing quantification, characterization and, in some cases, identification of the phase responsible for each resonance within the spectrum.

Due to the nonideal nature of the reaction products, it is not immediately possible to define the cations and/or anions present in each neophase. Therefore, it is also not possible to predict the exact overall ^{27}Al NMR shift observed for each phase based on presumed phase identity. Thus we must make reference to other spectroscopic data for assignment of the resonances in the ^{27}Al MAS NMR spectra. DRIFT spectra of specimen kaolinite reacted for 33 d along with the corresponding ^{27}Al NMR spectra are shown in Figure 5. The DRIFT spectrum of the unreacted clay displays a series of stretching motions in the 400−1200 cm^{-1} range and in the 3600−3800 cm^{-1} range. The band at approximately 3600 cm^{-1} is assignable to inner-hydroxyl groups of kaolinite at the base of the tetrahedral cavity.[29] Previously, a broad band at 3400 cm^{-1} has been observed that was attributable to hydrogen bonded water in the system. Between 950 and 1200 cm^{-1}, the series of absorptions correspond to Si−O−Si vibrational stretches. A strong absorption was also observed at 920 cm^{-1}, which is assignable to hydroxide bending vibrations of inner hydroxyl groups.[30] Upon increasing the STWL contact time at all Cs and Sr concentrations, the DRIFT spectra of the resulting complex mixture of parent clay and neophases change markedly. First, a broad band within the 2600−3600 cm^{-1} range develops intensity that increases with decreasing Cs and Sr concentration. It is highly

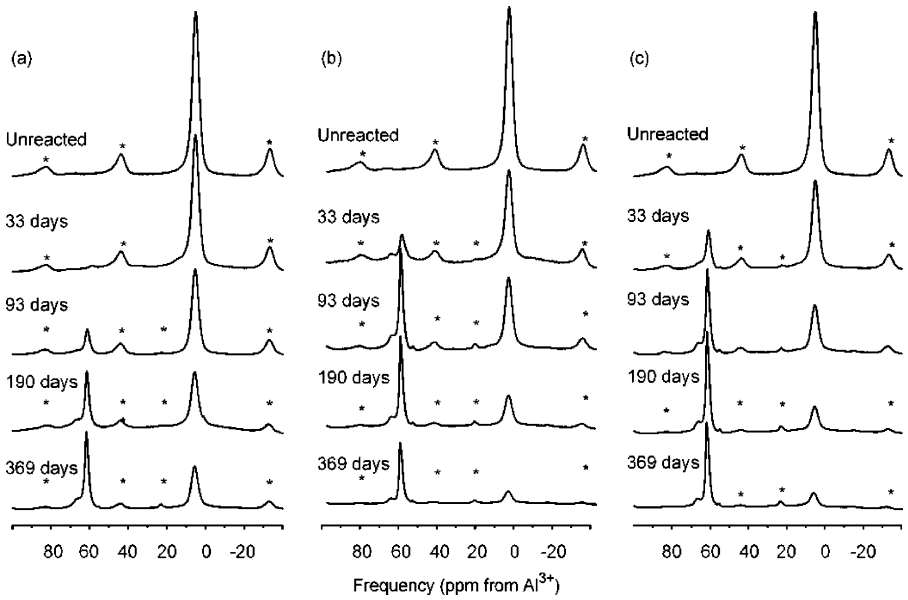

Figure 4. ^{27}Al MAS spectra obtained at 17.6 T from unreacted kaolinite and samples reacted for various times with the synthetic tank waste leachate solution at Cs/Sr concentrations of (a) 10^{-3}, (b) 10^{-4}, and (c) 10^{-5} *m*. Asterisks signify spinning sidebands in these MAS spectra.

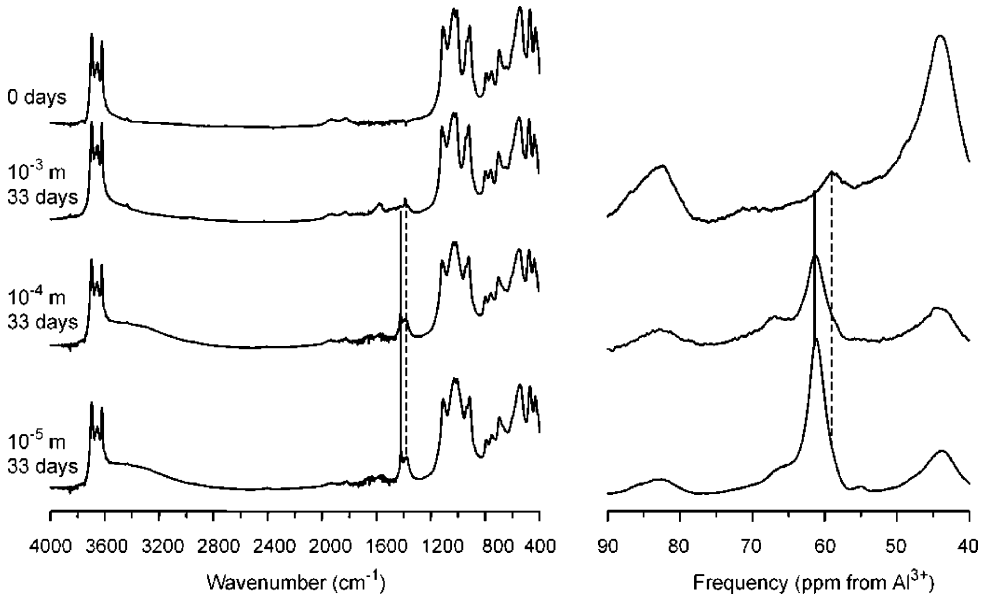

Figure 5. DRIFT and ^{27}Al NMR (obtained at 17.6 T) spectra of unreacted and 33 d reacted clays across the range of Cs/Sr concentrations. The dashed lines at approximately 1380 cm^{-1} and approximately 59 ppm represent the stretching vibration of the nitrate anion in sodalite cage of sodalite and the NMR resonance frequency of framework four-coordinate aluminum in sodalite, respectively. Upon decreasing the Cs/Sr concentration in the synthetic tank wash leachate solution, an additional peak is observed at 1420 cm^{-1} in the DRIFT spectra along with multiple resonances in the NMR spectra.

probable that this band results from incorporation of structural water into the newly formed phases. Additionally, sharp peaks develop between 1430 and 1370 cm^{-1}. After 33 d of STWL reaction and at 10^{-3} *m* Cs/Sr, a single peak forms around 1380 cm^{-1}; this peak is denoted with a dashed line in Figure 5 and is present at all concentrations of Cs and Sr. The band at 1384 cm^{-1} is characteristic of nitrate stretching vibrations.[30] At 10^{-4} and 10^{-5} *m* Cs/Sr, a peak is present at approximately 1424 cm^{-1}, also characteristic of nitrate stretching vibrations, albeit in a different local environment. The emergence of these peaks correlates with the development of new aluminum environments observed in ^{27}Al MAS NMR spectra in Figure 5. At 33 d and 10^{-3} *m* Cs/Sr, a small, although observable, feature is present in the MAS spectrum at around 59 ppm (denoted by the dashed line). This feature is broad, arguing for the presence of aluminum in a disordered phase. At lower concentrations of Cs and Sr, additional features are observed in the MAS spectra. At 10^{-4} *m* Cs/Sr, a broad resonance has developed at 68.1 ppm along with a sharp resonance at 62.3 ppm. The resonance observed at 33 d at 10^{-3} *m* may also be present as the shoulder observed in this spectrum, but the signal intensity is low. The observed ^{27}Al spectrum is also complex at the lowest dosage utilized in the study (10^{-5} *m* in Cs and Sr) with four resonances observed. As described below, the best spectral fits describe resonances with centers of gravity at 54.9, 62.6, 62.7, and 67.5 ppm.

Three phases (cancrinite, sodalite, and chabazite) were identified via XRD analyses after 190 d of STWL contact at all concentrations of Cs and Sr co-contamination.[6] In that study, the detection and quantification of these phases at early reaction times via XRD was hindered by the inherent inability of diffraction techniques to detect noncrystalline or low-abundance materials.[6] High-field NMR of quadrupolar nuclei in these

environments has no such limitation. Indeed, neophases were detected as early as 33 d in our ^{27}Al MAS experiments along with the growth of nitrate peaks in DRIFT spectra. The peaks observed in the high-field solid-state NMR spectra are assigned as follows. After 33 d, the phase detected at the highest co-contaminant dosage at 59 ppm contains nitrate, yet is an amorphous or poorly crystalline phase, possibly a precursor to sodalite. This assignment is based, in part, on the observation of the nitrate stretching band at 1384 cm^{-1} in the DRIFT spectrum, which is consistent with nitrate-sodalite. Scanning electron micrographs also showed particles consistent with sodalite morphology at 33 d.[6] We note that at lower contaminant ion concentrations at 33 d, a similar ^{27}Al peak is not strongly present, and an additional (narrower) peak appears with an overall shift at this field strength of approximately 62.9 ppm. At 10^{-4} and 10^{-5} *m*, the major resonances between 62 and 63 ppm are assigned to cancrinite and sodalite, and this assignment is based on the presence of an additional nitrate stretching band observed at 1424 cm^{-1}, which has been used by others as a diagnostic indicator for nitrate in a cancrinite phase.[19] Final distinction between these phases is made via comparison of relative peak intensities in the X-ray diffractograms at longer reaction times with the intensities of the peaks in the subsequent NMR spectra. For the samples reacted with STWL containing 10^{-3} *m* Cs and Sr co-contaminants, sodalite is the predominant species detected throughout the reaction sequence, and thus correlates strongly with the peak observed at 62.7 ppm.

Two additional resonances appear in the spectra at 33 d (and subsequently) and have not yet been identified. A high-frequency resonance (at approximately 68 ppm) is observed at the 10^{-4} and 10^{-5} *m* concentrations of Cs and Sr, while at the lowest concentration studied another phase is indicated by a peak at 54.9 ppm. Either of these peaks could arise from an amorphous aluminum-containing phase, and hence would not be observed via diffraction methods due to lack of long-range order. Alternatively, one of these two peaks could correspond to the small amounts of aluminum-rich chabazite inferred from the position of weak lines in the X-ray diffractograms at longer reaction times. While no reference could be found in the literature describing ^{27}Al NMR resonances from an Al-rich chabazite system, Akporiaye used ^{27}Al MAS NMR to study a series of pure chabazite phases with Si/Al ratios ranging from 2.6 to 12.6 and found that as the ratio increased the observed chemical shift generally decreased.[15] The observed chemical shift for a chabazite phase with a Si/Al ratio of 2.6 at 300 MHz was observed to be at 57.5 ppm, which is not inconsistent with previous low-field work performed in our lab.[6] Hence, a tentative assignment of this neophase resonance at 54.9 ppm is to the third phase described in our previous work as an Al-rich chabazite.

Deconvolutions of high-field ^{27}Al spectra were performed with DMFIT2002,[24] and integrated spectral intensities for each resonance at each time point were used to follow kinetics of the transformation processes. All ^{27}Al spectral deconvolutions were performed initially by using half-integer quadrupolar line shapes to fit peaks within the tetrahedral region (whereas ^{29}Si resonances were accomplished by using a mixture of Gaussian and Lorentzian line shapes), but most peaks appeared symmetric in shape, thus masking the evaluation of quadrupolar parameters by these methods but providing the center of gravity for each resonance. The observed shifts obtained from these deconvolutions were used to calculate the P_q and δ_{cs}^{iso} for each phase. Figure 6 depicts examples of ^{27}Al MAS spectral deconvolutions obtained at multiple fields along with individual components

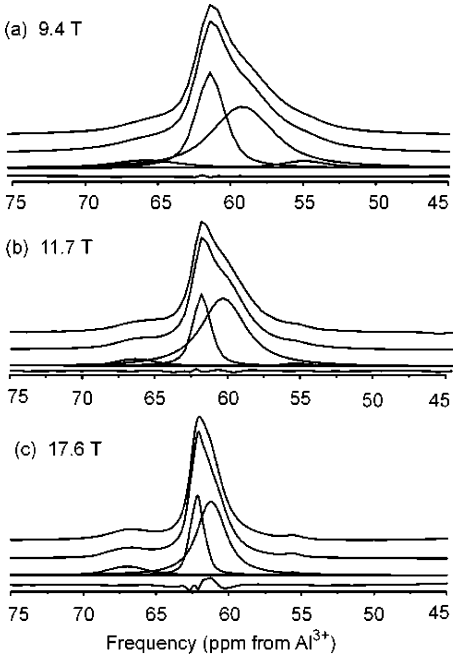

Figure 6. ^{27}Al Bloch decay spectra from kaolinite reacted for 365 d with a STWL containing 10^{-5} *m* Cs and Sr concentrations at (a) 9.4, (b) 11.7, and (c) 17.6 T. All spectra are displayed above a fit and the corresponding deconvolution of each spectrum with residuals shown below. All fits were performed with DMFIT2002.

and residuals for a sample of kaolinite reacted with STWL for 369 d with co-contaminant Cs and Sr concentrations of 10^{-5} *m*. From the deconvolutions of the individual spectra, we see that the three components with higher shift values all narrow and undergo a shift to higher frequency as the magnetic field strength increases, both of which indicate an operative quadrupolar interaction. The peak at the lowest observed shift value does not move significantly downfield, suggesting a small quadrupolar interaction. P_q and δ_{cs}^{iso} for all tetrahedral aluminum sites are listed in Tables 1 and 2 of the Supporting Information. P_q values for the neophases ranged from 0.4 MHz for the lowest frequency peak (after 369 d at 10^{-4} *m* Cs/Sr concentrations) to as high as 2.4 MHz for sodalite (after 369 d at 10^{-5} *m* Cs/Sr concentrations).

Silicon transformation from kaolinite to neophases is reported in Figure 7a as the percentage of the total silicon observed by NMR that remains present within the kaolinite resonance. At the highest co-contaminant concentration studied, silicon transformation was severely hindered initially with a maximum transformation of approximately 13% obtained after 190 d. However, the percentage of silicon transformed at lower co-contaminant concentrations (10^{-4} and 10^{-5} *m* Cs and Sr) after 190 d was 33% and 28%, respectively. Errors in these data are estimated at approximately ±3%, as the signal-to-noise ratios of these data are reasonable and allow reproducible deconvolutions. However, after 369 d of exposure, the signal-to-noise and spectral overlap of the ^{29}Si spectra were severe enough to preclude accurate quantification.

Figure 7b reports the percentage of total aluminum detected in the ^{27}Al MAS spectrum that remains within kaolinite, after contact with the STWL for the specified amount of time and at different Cs/Sr concentrations. Again, errors are estimated as ±3% at times longer than 0 d of exposure. Different Cs and Sr concentrations also affect the transformation of octahedral aluminum to neophases in this system. At 10^{-3} *m* Cs/Sr the transformation is again slower than that observed for lower concentrations, especially at short reaction times (33 d). In the

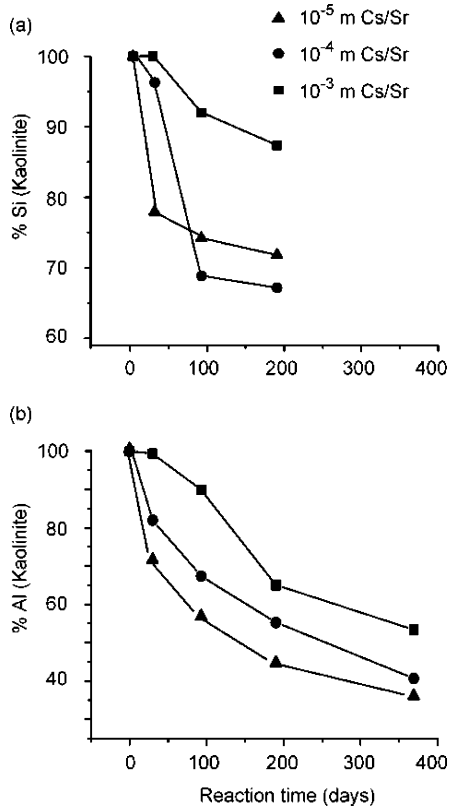

Figure 7. Time-dependent dissolution of kaolinite resonances from (a) ^{29}Si MAS spectra of STWL reacted kaolinite (1−190 d) at 10^{-3}, 10^{-4}, and 10^{-5} *m* Cs and Sr. (b) ^{27}Al MAS NMR spectra of time-dependent dissolution measured at 17.6 T for kaolinite at 10^{-3}, 10^{-4}, and 10^{-5} *m* Cs and Sr in the STWL for up to 369 d.

case of 10^{-4} and 10^{-5} *m* co-contaminant concentrations, the degree of transformation follows similar, but not identical, trends. The results of these studies indicate that Cs and Sr also play an important role in the transformation of octahedral aluminum, although not all Al in these studies arises from dissolution of the clay as the STWL initially contains 50 mmol kg^{-1} of total aluminum. Reported measurements of dissolved aluminum (and silicon) as a function of reaction time,[6] coupled with the results from quantitative NMR analyses, will enable a more detailed kinetic analysis for this complex process than described below, and these analyses are in progress. Here we focus on the quantification of the resulting species, and discuss the chemistry leading to such complex reaction kinetics.

The ^{27}Al MAS NMR spectra reveal the formation of four major aluminum-containing phases in this system as kaolinite dissolves. According to Ostwald's rule of phase transformation, the phase that forms first will be the least thermodynamically stable, followed by other phases in order of increasing phase stability. In our system, this argument would assert that the earliest sodalite-type phase formed is the least stable (although we cannot rule out a kinetically driven process), and sodalite is detected first via DRIFT and high-field NMR spectroscopies. Cancrinite most likely forms via a secondary nucleation process of sodalite,[17] but it is not proven here whether sodalite is required in this specific system for cancrinite to form. In fact, the sodalite-cancrinite mineral group contains a large number of related phases and characterization of these phases as representative end-member species could be misleading in this complex system. Spectroscopic evidence indicates the presence of small, disordered, and highly hydrated phases at 33 d and 10^{-3} *m* co-contaminant concentrations, which likely corresponds

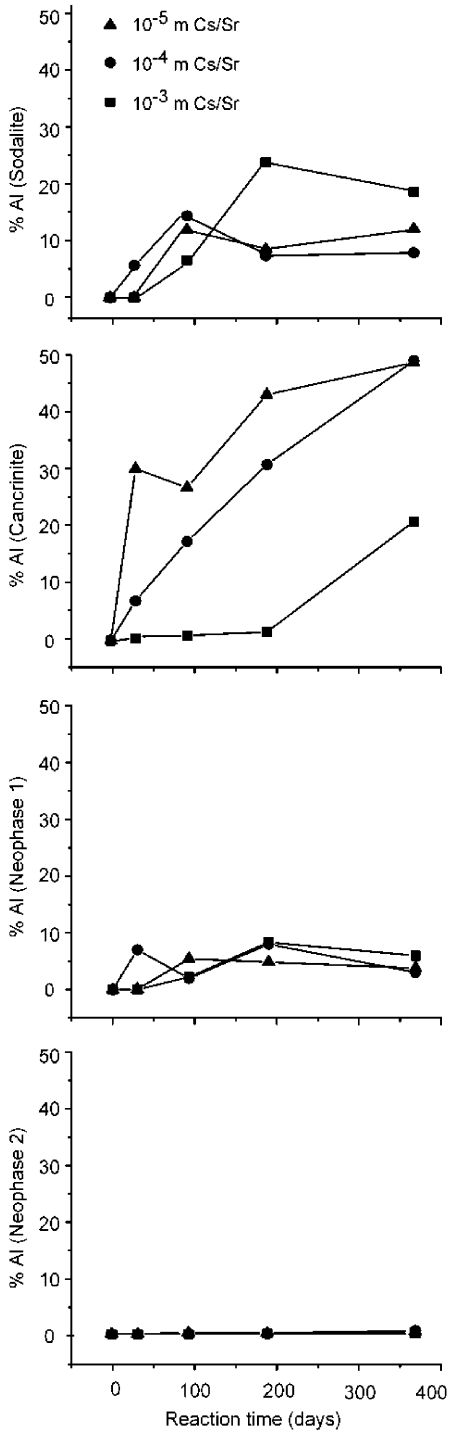

Figure 8. Time dependent formation of four-coordinate aluminum as detected by ^{27}Al MAS at 17.6 T in kaolinite systems reacted for up to 369 d with a STWL solution.

to the resonance at 59 ppm in the ^{27}Al MAS NMR spectrum of this sample. The contributions of each phase to the overall aluminum intensity after reaction with the STWL are detailed in Figure 8; however, the results at less than 93 d do not reflect small amounts of less-crystalline precursors that may also be present. Generally, errors here are difficult to quantify but probably lie in the range of ±3% when signal-to-noise ratios are sufficient.

The transformation of aluminum into various phases shows remarkable differences, and a full kinetic analysis is underway. In the case of sodalite formation, the change is slow at all concentrations up to 93 d after which there is an apparent

increase in the rate for the 10^{-3} *m* Cs/Sr system. At the last time point used in the study, the percentages of sodalite (as aluminum) at 10^{-4} and 10^{-5} *m* Cs/Sr are similar but less than that observed for the highest concentration studied here. The influence of Cs and Sr on the formation of cancrinite at all concentrations indicates that at high concentrations the rate of formation of the phase slightly increases up to 190 d, after which a large rate change occurs with the percentage of aluminum as cancrinite jumping from less than 5% to approximately 17.5%. For cancrinite formation at lower Cs and Sr concentrations, we observe greater increases in the percentages with increasing solution contact time as the co-contaminant concentration decreases. The other yet to be identified neophases, referred to as neophase 1 (at 67.5 ppm when the magnetic field strength is 17.6 T) and neophase 2 (at 54.9 ppm, and possibly the phase corresponding to Al-rich chabazite), show very little growth over the time span of the experiments. In fact, in both cases, neither phase contributes more than 10% of the total signal at the longest reaction times.

The formation rate of cancrinite in these weathered systems is closely related to the initial concentrations of Cs and Sr. At the highest Cs and Sr dosage utilized, cancrinite development is hindered by the rate of sodalite growth (as detected by ^{27}Al MAS NMR). However, beyond 190 d, there is a decrease in the relative amount of sodalite and the percentage of cancrinite increases from 1% to nearly 20%. At concentrations of Cs and Sr less than 10^{-3} *m*, cancrinite also forms at the expense of sodalite. After 33 d at 10^{-4} *m* Cs and Sr, both sodalite and cancrinite are detectable via NMR analyses while at the same time point at 10^{-5} *m* Cs and Sr, sodalite was not observed in the presence of cancrinite. At reaction times up to 93 d at the 10^{-4} and 10^{-5} *m* Cs and Sr, sodalite formation is not diminished as cancrinite forms; however, beyond 93 d, a decrease in the relative amount of sodalite occurs.

At the highest Cs and Sr concentration in our STWL solutions, the rate of kaolinite dissolution (as measured via ^{29}Si and ^{27}Al MAS NMR) is severely hindered relative to lower contaminant concentrations. A possible explanation for this observation could be the formation of Sr-containing solids. In a companion study, Sr K-edge EXAFS was used to examine changes in the local bonding environment around Sr as the reacted kaolinite samples aged.[31] At Sr and Cs concentrations of 10^{-3} *m*, EXAFS spectra of Sr at 1 and 7 d indicate the formation of a Sr phase with the local structure of $SrCO_3$(s). Although CO_2 was excluded from the reactant solutions, diffusion of ambient CO_2 into solutions during reaction was not prevented. We estimate that the solubility of $SrCO_3$(s) was exceeded at Sr = 10^{-3} *m*, but not at 10^{-4} or 10^{-5} *m*. The $SrCO_3$(s) phase was not detected by XRD or SEM/TEM, suggesting that particle size is very small and particles may form as surface coatings. Spectral evidence for this phase is weak in the Sr EXAFS at 33 d, indicating that it is transient or of low relative abundance compared to increasing amounts of emerging aluminosilicate phases that sequester Sr.[31] The formation of a surface precipitate at early reaction times may retard the kaolinite dissolution rate at 10^{-3} *m* by blocking surface sites to hydroxide attack. At lower Sr concentrations in the absence of a carbonate precipitate, Sr may adsorb to the kaolinite surface as a hydrated surface complex.[32] Measurements of the temporal evolution of dissolved Sr^{2+} in our system showed that at all concentrations, rapid uptake occurred at 1 and 7 d.[6] The formation of a surface precipitate at 10^{-3} *m* Sr but adsorption of surface complexes at 10^{-4} and 10^{-5} *m* may explain the slower kaolinite dissolution rate (determined from Si release) at higher Sr and Cs concentrations during early reaction times (up to 33 d).

The formation of new feldspathoid phases from kaolinite dissolution under STWL conditions appears coupled closely to the uptake of Cs and Sr. Sodalite group phases such as cancrinite and sodalite are known sorbents for Cs,[33−36] although these phases can also incorporate divalent cations. In all likelihood, the reaction responsible for the formation of stoichiometric nitrate-cancrinite and nitrate-sodalite is

$$6Al(OH)_4^- + 6H_2SiO_4^{2-} + 8Na^+ + 2NO_3^- \rightarrow Na_6Si_6Al_6O_{24}\cdot 2NaNO_3 + 12OH^- + 12H_2O \quad (I)$$

In nature, the charge balancing cation present when cancrinite and sodalite forms is Na^+, but Cs^+ can be incorporated into the mineral structure via an exchange reaction with Na^+.[6,33]

In contrast to Sr^{2+} uptake from solution, which was rapid relative to the time scale of the formation of zeolite-like minerals (as detected by ^{27}Al NMR), Cs^+ removal from solution was gradual and qualitatively followed the development of four-coordinate aluminum in our systems. At low co-contaminant concentrations, the formation of cancrinite is gradual up to 190 d (see Figure 8); this tracks with the removal of Cs from the solution.[6] At the other concentration extreme studied here, the removal of Cs does not follow the formation of either sodalite or cancrinite. Thus it is possible that the cation is being distributed among both phases. Mixed-cation cancrinite has been observed in the presence of large and small cations such as Cs^+ and Na^+, suggesting that a mixed-cation cancrinite (or sodalite) could be forming in these systems.[37]

Conclusions

The hydroxide-promoted reaction of kaolinite under conditions similar to those found near leaking storage tanks at the Hanford Site in southeastern Washington was studied via ^{29}Si NMR and multiple-field ^{27}Al NMR. The transformation rates of kaolinite as measured by quantitative NMR exhibited an inverse dependence on the initial dosages of Cs and Sr. Using high-field ^{27}Al MAS NMR we were able to observe, characterize, and quantify (for the first time), the time evolution of four distinct aluminum-containing phases (in addition to the parent kaolinite). Two of these phases are identified as feldspathoid minerals cancrinite and sodalite, both of which are extremely important sorbents of Cs and Sr. Formation of these end-member phases in the sodalite-cancrinite family is preceded by the presence of one or more less-crystalline phases, from which we detect an ^{27}Al resonance at 33 d under conditions of high co-contaminant concentrations. A comparison of Sr removal from solution to that of Cs showed that the concentration of Sr rapidly decreased (after 1 d) at all concentrations while the removal of Cs was more gradual and appeared to track quantitatively with the formation of feldspathoid phases. These observations point toward a coupling of Cs sorption to the ripening of feldspathoid phases in heterogeneous systems that, with increasing time, provide more cation sites for Cs. These results also exemplify the potential interacting influence of co-contaminants, an effect that is rarely appreciated. In this case, surface precipitation of one contaminant ion (Sr^{2+}) has diminished the rate of growth of a high affinity sorbent for Cs, thereby affecting the rate of solid-phase sequestration of this second contaminant ion. When combined with the results of our prior study,[6] the data suggest that rapid strontium uptake to the kaolinite surface diminished the hydroxide-induced rupture of

critical bridging bonds within Si−O−Al units and also within Si−O−Si and Al−O−Al units.

Acknowledgment. This research was supported under the United States Department of Energy's Environmental Management Science Program, grant DE-FG07-99ER15012. Support was also provided to G.S.C. by the U.S. EPA via the Science to Achieve Results (STAR) Fellowship Program, grant U91612401. Part of this research was performed at the Environmental Molecular Sciences Laboratory (EMSL), a national scientific user facility sponsored by the U.S. DOE Office of Biological and Environmental Research, located at Pacific Northwest National Laboratory, operated by Battelle for the DOE. We would like to thank Dr. David Hoyt, Dr. Joseph Ford, and the EMSL staff for their kind assistance and for access to their facility, without which this work would not have been possible. The authors also thank Michael Davis at PSU for assistance with data acquisition. The NMR spectrometers used within the Penn State NMR Facility were acquired with assistance from the National Science Foundation through grants CHE-9601572 and DMR-9413674.

Supporting Information Available: Tables giving a summary of peak shifts from deconvoluted ^{27}Al MAS NMR data and calculated isotropic chemical shift and quadrupolar product for each major and minor phase in this study. This material is available free of charge via the Internet at http://pubs.acs.org.

References and Notes

(1) Gephart, R. E.; Lundren, R. E. *Hanford tank cleanup*: *a guide to understanding the technical issues*; Battelle Press: Columbus, OH, 1998.

(2) Behrens, E.; Sylvester, P.; Clearfield, A. *Environ. Sci. Technol.* **1998**, *32*, 101−107.

(3) Bauer, A.; Velde, B.; Berger, G. *Appl. Geochem.* **1998**, *13*, 619−629.

(4) Bickmore, B. R.; Nagy, K. L.; Young, J. S.; Drexler, J. W. *Environ. Sci. Technol.* **2001**, *35*, 4481−4486.

(5) Zhao, H. T.; Deng, Y. J.; Harsh, J. B.; Flury, M.; Boyle, J. S. *Clay Clay Min.* **2004**, *52*, 1−13.

(6) Chorover, J.; Choi, S.; Amistadi, M. K.; Karthikeyan, K. G.; Crosson, G.; Mueller, K. T. *Environ. Sci. Technol.* **2003**, *37*, 2200−2208.

(7) Komarneni, S.; Fyfe, C. A.; Kennedy Gordon, J. *Clay Min.* **1985**, *20*, 327−334.

(8) Fitzgerald, J. J.; Hamza, A. I.; Bronnimann, C. E.; Dec, S. F. *J. Am. Chem. Soc.* **1997**, *119*, 7105−7113.

(9) Benharrats, N.; Belbachir, M.; Legrand, A. P.; De La Caillerie, J. B. D. E. *Clay Min.* **2003**, *38*, 49−61.

(10) Begin, L.; Fortin, J. *J. Environ. Qual.* **2003**, *32*, 662−673.

(11) Barron, P. F.; Frost, R. L.; Skjemstad, J. O.; Koppi, A. J. *Nature* **1983**, *302*, 49−50.

(12) Hayashi, S.; Ueda, T.; Hayamizu, K.; Akiba, E. *J. Phys. Chem.* **1992**, *96*, 10922−10928.

(13) Bish, D. L.; Vondreele, R. B. *Clay Clay Min.* **1989**, *37*, 289−296.

(14) Flanigen, E. In *Introduction to Zeolite Science and Practice*, 2nd ed.; Elsevier: Amsterdam, The Netherlands, 2001; Vol. 1, pp 11−32.

(15) Akporiaye, D. E.; Dahl, I. M.; Mostad, H. B.; Wendelbo, R. *J. Phys. Chem.* **1996**, *100*, 4148−4153.

(16) Lippmma, E.; Samoson, A.; Tarmak, M.; Engelhardt, G. *J. Am. Chem. Soc.* **1981**, *103*, 4992−4996.

(17) Barnes, M. C.; Addai-Mensah, J.; Gerson, A. R. *Microporous Mesoporous Mater.* **1999**, *31*, 303−309.

(18) Buhl, J. C. *Thermochim. Acta* **1991**, *189*, 75−82.

(19) Buhl, J. C.; Stief, F.; Fechtelkord, M.; Gesing, T. M.; Taphorn, U.; Taake, C. *J. Alloy. Compd.* **2000**, *305*, 93−102.

(20) Buhl, J. C. *Thermochim. Acta* **1996**, *286*, 251−262.

(21) Wieland, E.; Stumm, W. *Geochim. Cosmochim. Acta* **1992**, *56*, 3339−3355.

(22) Jones, R. C.; Babcock, C. J.; Knowlton, W. B. *Soil Sci. Soc. Am. J.* **2000**, *64*, 1100−1108.

(23) Acebal, S. G.; Mijovilovich, A.; Rueda, E. H.; Aguirre, M. E.; Saragovi, C. *Clay Clay Min.* **2000**, *48*, 322−330.

(24) Massiot, D.; Fayon, F.; Capron, M.; King, I.; Le Calve, S.; Alonso, B.; Durand, J. O.; Bujoli, B.; Gan, Z. H.; Hoatson, G. *Magn. Reson. Chem.* **2002**, *40*, 70−76.

(25) Temuujin, J.; Okada, K.; MacKenzie, K. J. D. *Mater. Lett.* **2002**, *52*, 91−95.

(26) Gualtieri, A. F.; Norby, P.; Artioli, G.; Hanson, J. C. *Phys. Chem. Miner.* **1997**, *24*, 191−199.

(27) Nagy, K. L. In *Chemical Weathering Rates of Silicate Minerals*; Mineralogical Society of America: Washington, DC, 1995; Vol. 31, pp 173−233.

(28) Devidal, J. L.; Schott, J.; Dandurand, J. L. *Geochim. Cosmochim. Acta* **1997**, *61*, 5165−5186.

(29) Rotenberg, P. M.S. Thesis, Penn State University, 2002.

(30) Farmer, V. C. *The Infrared Spectra of Minerals*; Minerological Society: London, UK, 1974; Vol. 4.

(31) Choi, S.; O'Day, P. A.; Rivera, N. A.; Mueller, K. T.; Vairavamurthy, M. A.; Seraphin, S.; Chorover, J. *Environ. Sci. Technol.* **2005**, submitted for publication.

(32) Sahai, N.; Carroll, S. A.; Roberts, S.; O'Day, P. A. *J. Colloid Interface Sci.* **2000**, *222*, 198−212.

(33) Ahn, M. K.; Iton, L. E. *J. Phys. Chem.* **1989**, *93*, 4924−4927.

(34) Anchell, J. L.; White, J. C.; Thompson, M. R.; Hess, A. C. *J. Phys. Chem.* **1994**, *98*, 4463−4468.

(35) Hunger, M.; Schenk, U.; Buchholz, A. *J. Phys. Chem. B* **2000**, *104*, 12230−12236.

(36) Freude, D.; Loeser, T.; Michel, D.; Pingel, U.; Prochnow, D. *Solid State Nucl. Magn. Reson.* **2001**, *20*, 46−60.

(37) Norby, P.; Krogh Anderson, I. G.; Krogh Anderson, E.; Colella, C.; de'Gennaro, M. *Zeolites* **1991**, *11*, 248−253.